Aerodynamic water droplet with strong lightweight bone structure

Engineering Design Research Laboratory
Indiana University-Purdue University Indianapolis
http://et2.engr.iupui.edu/~tovara/edrl/

Executive Summary

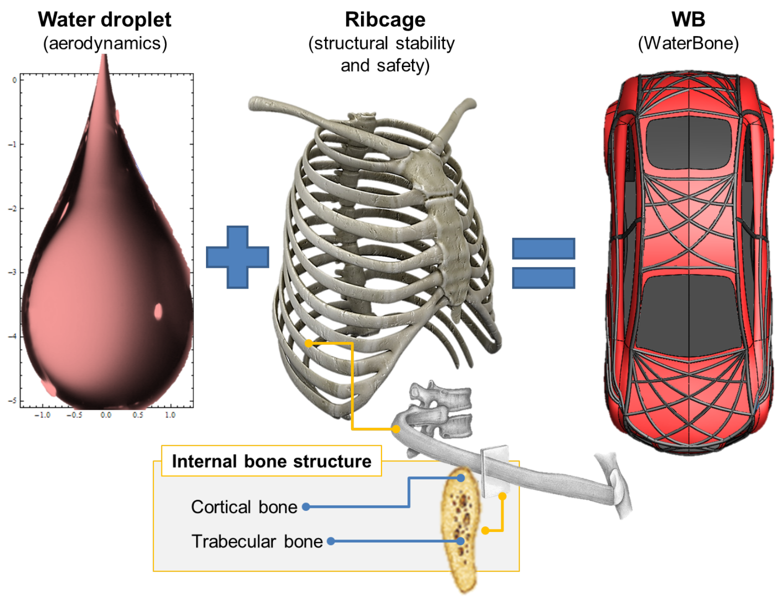

Figure 1: Graphical Abstract: The concept vehicle combines the shape of a water droplet and the spaceframe design similar to a ribcage. Each structural component has a graded porous structure similar to the one of a bone.

The proposed vehicle design has the shape of a **water droplet** with an embedded **ribcage** (Figure 1). The water droplet shape provides a low drag coefficient for higher fuel economy. The ribcage is designed with a graded porous structure, similar to the ones in bones. These structures provide the mechanical strength required for the structural stability and drivability as well as the energy absorption capabilities for the occupant safety in the event of a collision. The ribcage is built in functionally graded aluminum alloy foam, with the level of protection of a spaceframe design such as NASCAR racecar. The envelope's material is polymer composite, which provides desirable characteristics of a monocoque design traditionally found in Formula 1 cars and aircrafts. The monocoque-sapaceframe design is built using additive manufacturing (3D printing) technology, providing a cleaner an environmentally friendly operation with minimal material wastage. This design merges aerodynamics and safety. This concept design is referred to as WaterBone (WB).

Weight Reduction Methodology

The weight reduction in this design has been achieved in two ways: **material substitution** and **optimal design** of the shape (envelope) and the ribcage (spaceframe). The optimal structural layout has been obtained with the application of a specialized topology optimization algorithm for crashworthiness. The following sections explain in detail the optimization algorithms used in this design.

1. Topology optimization of lightweight components

In the automotive industry, topology optimization is being recognized as a viable approach to generate groundbreaking, lightweight conceptual designs [1]. Our topology optimization algorithm, referred to as hybrid cellular automata (HCA), has been originally proposed and developed by Dr. Tovar and collaborators with the support of Honda R&D Americas [2-8].

Currently, the HCA algorithm is implemented by Livermore Software Technology Corporation LSTC (Livermore, California) in their commercial finite element analysis (FEA) software LS-DYNA [9]. The topology optimization problem to be initially addressed is to find the material distribution $\mathbf{x}$ that maximizes the internal energy (IE) and subject to a mass (M) constraint. The mathematical problem statement is

$$\begin{aligned} &\text{find} && \mathbf{x} \in \mathbb{R}^n \\ &\text{maximize} && \mathrm{IE}(\mathbf{x}) = \int_0^{\Delta} P(\delta, \mathbf{x}) d\delta \\ &\text{subject to} && \mathrm{M}(\mathbf{x}) = \int_{\Omega} \rho(\mathbf{x}) d\Omega = M_0, \qquad x_i \in \{0,1\}, \qquad i = 1, \dots, n \end{aligned} \tag{1}$$

where $P(\delta, \mathbf{x})$ is the reaction force after a collision, Δ is the crushing distance, $\rho(\mathbf{x})$ is the material density, M_0 is the mass target, and Ω is the volume of the design domain where the material will be distributed. In this formulation, the design domain is discretized into n elements (voxels) so each voxel will have a value of solid when $x_i = 1$ or void when $x_i = 0$.

The two main difficulties of solving this problem using traditional optimization algorithms are the computational cost of the crash simulation needed to evaluate IE, and the lack of sensitivity coefficients needed to drive the optimization algorithm. To address these difficulties, design researchers have proposed some specialized topology optimization algorithms, which can be classified into four groups: (1) ground structures, (2) linear implicit methods, (3) partially non-linear implicit methods, and (4) truly non-linear explicit methods.

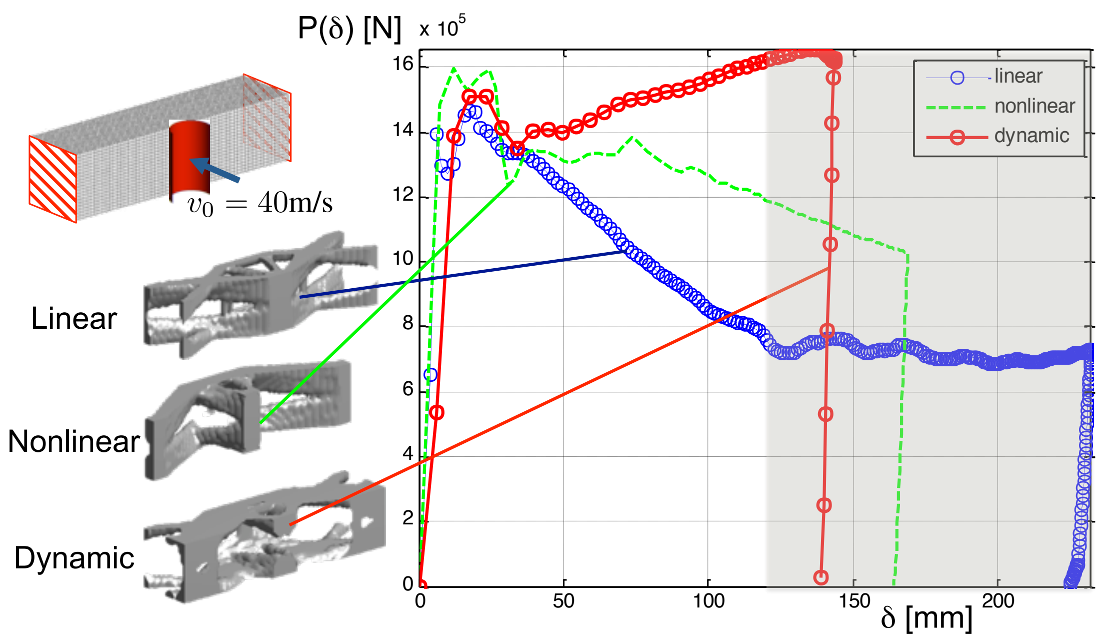

Figure 2: Topology optimization of a bumper structure using the HCA algorithm using three material models and loading cases: linear/static, nonlinear/static, and nonlinear/dynamic [4].

Algorithms based on ground structures [10, 11] rely on a design space filled with beam-type elements, which are sequentially deleted. Today, this rather coarse modeling of the structure has limited application. Algorithms based on linear implicit finite element analysis, such as equivalent static loads (ESL) [12, 13] or partially non-linear implicit methods [14, 15] are numerically efficient, since sensitivity coefficients can be obtained. Unfortunately, these approaches are unable to capture all the relevant aspects of the transient, dynamic crash event. Finally, truly non-linear explicit algorithms have been proposed by research groups at Ford [16] and Volvo [17], and also by PI Tovar's group and Honda (HCA) [2-8]. The main advantages of the HCA algorithm are the proven convergence [18], its convergence rate [19], and its extension to solve a variety of topology problems [20]. When applied to a single crashworthy vehicle component, say a bumper, the HCA algorithm finds the material distribution that maximizes IE for a given mass target (Figure 2). While these designs may be sufficient for some vehicle components, this current strategy is not applicable to the design of crumple zone in the front and rear ends of the vehicle.

2. <u>Design of lightweight energy absorbing, progressively folding components</u>

Besides IE and mass, other crashworthiness indicators must be considered, namely, specific energy absorption (SEA), mean crushing force (MCF), peak crushing force (PCF), crash load efficiency (CLE), and progressive folding. The SEA is defined as the ratio between IE and mass,

$$\mathrm{SEA}(\Delta, \mathbf{x}) = \frac{\mathrm{IE}(\Delta, \mathbf{x})}{\mathrm{M}(\mathbf{x})}$$

where $\mathrm{IE}(\Delta, \mathbf{x}) = \mathrm{MCF}(\Delta)\Delta$. In other words, the IE is the MCF multiplied by the crushing distance. The CLE is defined as

$$\mathrm{CLE}(\Delta, \mathbf{x}) = \frac{\mathrm{MCF}(\Delta)}{\mathrm{PCF}}$$

where PCF is the maximum value of the reaction force $P(\delta, \mathbf{x})$ during the crash event. Then, a more suitable design problem for crumple zones is as follows:

$$\begin{array}{ll}
\text{find} & \mathbf{x} \in \mathbb{R}^n \\
\text{maximize} & \mathrm{SEA}(\Delta, \mathbf{x}) = \dfrac{\mathrm{IE}(\Delta, \mathbf{x})}{\mathrm{M}(\mathbf{x})} = \dfrac{\int_0^{\Delta} P(\delta, \mathbf{x}) d\delta}{\int_{\Omega} \rho(\mathbf{x}) d\Omega} \\
\text{minimize} & \mathrm{PCF} = \max P(\delta) \\
\text{maximize} & \mathrm{CLE}(\Delta, \mathbf{x}) \\
\text{subject to} & x_i \in \{0,1\}, \qquad i = 1, \dots, n
\end{array} \tag{2}$$

In order to address this crashworthiness problem, we have proposed a design algorithm that uses the “gray” design generated by HCA that is then clustered and optimized using sequential metamodel-based genetic programming [21]. The multiscale design offers an optimal spaceframe design that maximizes internal energy, Eq. (1), and the internal functionally graded cellular structure to manage the impact by extremizing crashworthiness indicators, Eq. (2). The loading conditions for the optimal space frame two frontal pole impacts (full frontal and offset) and three side impacts (central and two offsets) (Figure 3). The result is a lightweight structure that satisfies all safety standards.

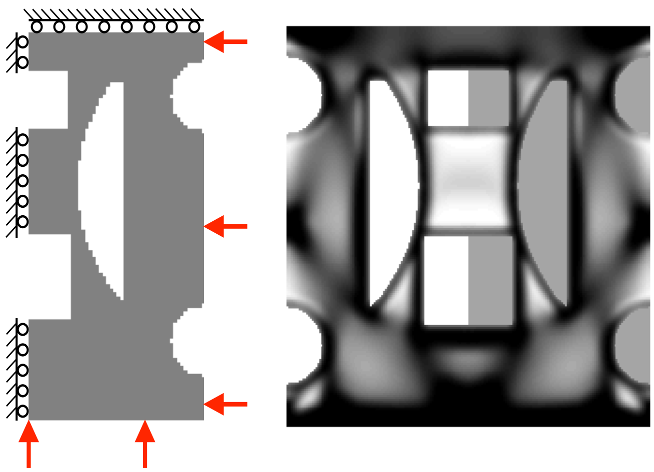

Figure 3: Functionally graded cellular structure distribution as a result of five loading conditions

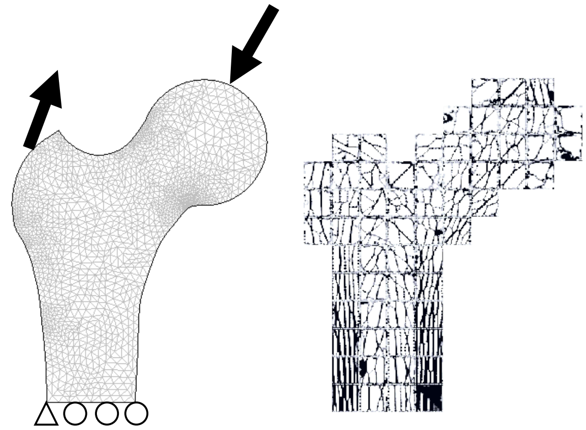

Figure 4: Internal structure generated with the HCA topology optimization algorithm.

Innovation

The proposed design has outstanding differences from the current state-of-the-art in vehicle design in terms of the structural layout, use of multi-materials, and the 3D printing manufacturing process.

1. <u>Novel multiscale structural layout</u>

The topology optimization algorithm used in this design generates innovative lightweight layouts with high crashworthiness indicators. The unique HCA topology optimization algorithm has the ability to generate multiscale designs. At the vehicle scale, the generated spaceframe has a structure similar to the one of long bone. In essence, the aerodynamic water droplet shape is protected by specialized ribcage that follows principles of Michell-type structures [22]. At the component scale, each spaceframe tubular component is filled with a functionally graded cellular structure. This internal cellular structure reminds the one of a bone (Figure 4). Also, the spaceframe is attainable with very few parts of greater complexity. Such complex, lightweight, multiscale structural layout is manufacturable using 3D printing technologies.

2. <u>Novel lightweight multi-material design</u>

Our design proposes to substitute the metal sheets of the extensively used unibody structure for a metallic space frame and lightweight polymer composite envelope. The envelope's polymer composite provides desirable safety characteristics of a monocoque design traditionally found in Formula 1 cars and aircrafts. The metallic (functionally graded cellular) spaceframe provides a level of protection similar to racercars that also use sapceframe design, such as NASCAR car. However, the proposed design has less than 50% its weight with significantly lower part count. The result is a design of very light, strong, and safe (crashworthy) components with the possibility of utilizing a wide variety of plastics and metals and, hopefully, more environmentally friendly materials that are 100% recyclable (Figure 5).

3. Novel manufacturing process

The freedom in the multi-scale/multi-material design is possible due to the benefits of 3D printing technologies. Besides providing lightweight and innovative vehicle designs, 3D printing offers a number of benefits in comparison to current manufacturing processes. In comparison to metal sheet processing, 3D printing holds the promise of cleaner and environmentally friendlier operation that allows complex part production with minimal overall material wastage. 3D printing allows free-form mass customization with reduced time to market and low overall cost. From the Lamborghini Lab, the cost comparison between traditional manufacturing process and 3D printing with fuse deposition modeling (FDM) technology, it is expected to have a 93% reduction in the manufacturing cost and 83% reduction in manufacturing cycle time (Figure 6)[1]. The use 3D printing offers the possibility to consolidate parts and reduce the design complexity in terms of part count. Finally, there is a staggering number of plastics and metal alloys suitable for several 3D printing technologies. Therefore, the use of 3DP plastics and 3DP metals supports vehicle material substitution and facilitates vehicle lightweighting.

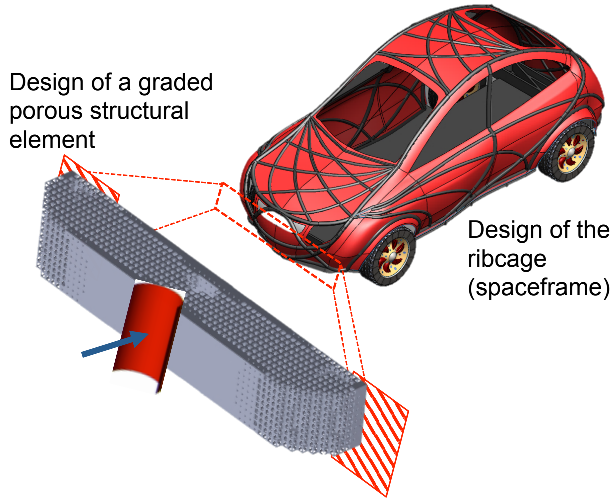

Figure 5: Final design of the metallic spaceframe (left) and the polymer composite envelope (right)

How does FDM compare with traditional processes for Lamborghini Lab?

Method	Cost	Time
Traditional process	$40,000	120 days
FDM Technology	$3,000	20 days
SAVINGS	**$37,000 (93%)**	**100 days (83%)**

Figure 6: Cost comparison between traditional manufacturing and 3D printing (FDM)

Bill of Materials

The two material used in this design are reinforced ABS (ABS) and AlSi10Mg alloy (AL). The cost of 3D printing AL is $56 per cubic inch (powder sintering). The cost of 3D printing ABS in pellet form (big area additive manufacturing) is $1 per pound. The average density of the cellular AL (foam) is 0.0490 lb/in3. The density of ABS is 0.0397 lb/in3. The average diameter of the AL tube is 2.0 in. The average thickness layer of ABS is 0.25 in. The total weight of the structure is 295 lb (63% AL, 37 ABS). The total cost of the structure is estimated in $212k (Table 1).

Table 1: Details of the Bill of Materials

Part	Quantity	Weight [lb]	% W AL	% W ABS	Cost
Frame	1	185	59%	41%	$125,984
Passenger front door	2	19	62%	38%	$13,290
Passenger back door	2	15	75%	25%	$12,847
Bonnet	1	20	78%	22%	$18,125
Back door	1	22	63%	37%	$15,666
Total	**7**	**295**	**63%**	**37%**	**$212,047**

[1] http://www.stratasys.com/resources/case-studies/automotive/lamborghini

Required Manufacturing Processes

The vehicle structure has a level of complexity that is suitable for 3D printing. The 3D printing process will be carried out in two stages. In the first stage, the functionally graded metallic spaceframe is printed in AlSi10Mg alloy using powder sintering or direct metal printing in a conventional inert argon or nitrogen atmosphere. In the second stage, the polymer composite layer is printed in reinforced ABS using big area additive manufacturing (BAAM). BAAM is a fused deposition modeling (FDM) process that uses pellet feed instead of the most commonly used filament. While the cost of filament run around $20 per kilogram, the cost of pellets is below $2 per kilogram. In addition, the use of pellets allows ABS reinforcements not available in filament form.

Passenger Safety

The crashworthiness of a vehicle design must be verified with numerical and physical tests that generally fall in of the following categories: component tests, sled impact test, and full-scale barrier impact test. Component tests are used to evaluate the impact energy management capabilities of the vehicles structural elements. Crashworthy structural elements, generally referred to as energy absorbers, can be classified into two categories: reversible energy absorbers such as hydraulic dashpots and elastic dampers, and irreversible energy absorbers, which include structural components that dissipate energy through plastic deformation. Our design makes use of lightweight irreversible energy absorbers (Figure 7).

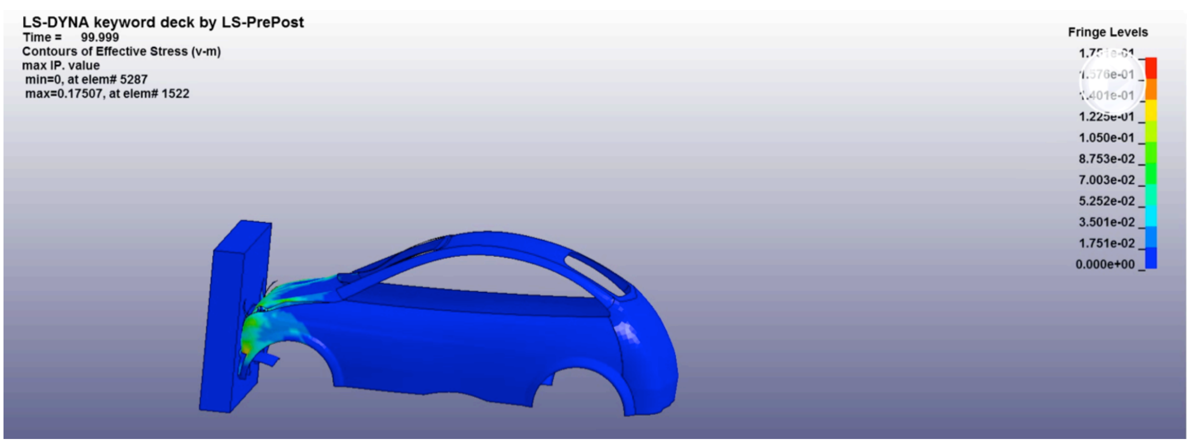

Figure 7: Effective plastic stress distribution in frontal impact simulated at 40 mph

Sled tests are used to evaluate restrain systems using cadavers or anthropomorphic tests devices. Such tests have not yet considered, but a suitable restrain system must be incorporated in this design. Finally, full-scale barrier impact tests involve the collision of a guided vehicle into a barrier to ensure occupant protection and vehicle structural integrity. These tests are regulated in our country by the Federal Motors Vehicle Safety Standard (FMVSS) and Regulations issued by the U.S. Department of Transportation's National Highway Traffic Safety Administration (NHTSA) [41, 42]. All crashworthiness indicators have been numerically verified using dynamic, non-linear finite elements analysis with LS-DYNA (LSTC, Livermore, California) using a full-scale barrrier impact. Three tests have been performed in our final design: full frontal impact, offset frontal impact with 40% overlap, and side impact. All tests have been done at 40 mph.

Innovative/Safety Component

The proposed design has several innovative and safety components. First, the envelope's water droplet shape provides low drag coefficient. The addition of a crumple zone decreases this coefficient but allows to dramatically increasing crashworthiness indicators. The expected drag coefficient of the proposed design car is 0.25, which is still lower than most sedans in the market, hence increases fuel efficiency. This decreases the engine size and the energy storage devices and increases the safety of the vehicle by reducing the risk of ignition. Second, the spaceframe of the vehicle is generated by topology optimization to provide strength minimizing the penetration of the cabin during a crash event and mantaining the structural integrity of the cabin in the same way a NASCAR racecar behaves. Third, the internal structure of each spaceframe tube is filled with functionally graded materials (just like our bones) so the structure can manage the impact kinetic energy with minimum weight and without scarifying crashworthiness performances. The design is tailored so crumpling zones progressively fold. Fourth, the use of polymer composite dissipates energy in the same way monochoque structures in Formula 1 do it increasing the safety of the design. The use of multiple materials and a systematic structural optimization algorithm helps this design to achieve levels of safety no attainable with one single material. In summary, the proposed vehicle design enables vehicle lightweighting with high safety standards.

Potential Challenges

1. Lack of material constitutive models

Potential challenge: Despite the increasing accessibility of 3D printing technologies to automakers and the growing number of suitable plastics and metals, there are very few studies that support experimentally validated 3D printed material constitutive models for crashworthiness. Therefore, the most outstanding challenge is the correctly model the performance of the 3D printed vehicle to accurately tailor its optimum design.

Proposed solution: To address this challenge, more research is needed to correctly characterize the 3D printed material performance under variable high-strain rates (10^2 to $10^3 \mathrm{s}^{-1}$). Our research laboratory is currently developing strain rate-sensitive constitutive models of 3D printed plastic (ABS P400) and 3D printed metal (AlSi10Mg alloy).

2. Manufacturing cost

Potential challenge: The cost of the 3D printing process for metal structure remains high. For instance, depending on the 3D printing technology, the cost of printing one cubic inch in stainless steel varies from $40 (powder sintering) to $80 (direct metal printing). The cost of 3D printing aluminum alloy is about 40% more expensive. Substantial initial investments and large 3D printing technology must be still incorporated by OEMs. Also, multi-material (metal/polymer) 3D printing technology requires development.

Proposed solution: As 3D printing technologies and material it is expected that these prices will dramatically drop. Furthermore, the overall cost of the vehicle will also decrease with the use of 3D printing. Currently, our research group works with a local company, 3D Parts Manufacturing, LLC (Indianapolis, Indiana) in the development of multi-material and metal powders for 3D printing technologies.

References

1. Bendsøe, M.P. and O. Sigmund, *Topology Optimization: Theory, Methods and Applications*. 2003: Springer.
2. Tovar, A., et al., *Topology optimization using a hybrid cellular automaton method with local control rules.* Journal of Mechanical Design, 2006. **128**(6): p. 1205-1216.
3. Tovar, A., et al., *Optimality conditions of the hybrid cellular automata for structural optimization.* AIAA Journal, 2007. **45**(3): p. 673-683.
4. Patel, N.M., et al., *Crashworthiness Design Using Topology Optimization.* Journal of Mechanical Design, 2009. **131**(6): p. 12.
5. Guo, L., et al., *Multidomain topology optimization for crashworthiness based on hybrid cellular automata.* Key Engineering Materials, 2011. **486**: p. 250-253.
6. Mozumder, C., J.E. Renaud, and A. Tovar, *Topometry optimisation for crashworthiness design using hybrid cellular automata.* International Journal of Vehicle Design, 2012. **60**(1-2): p. 100-120.
7. Bandi, P., J.P. Schmiedeler, and A. Tovar, *Design of Crashworthy Structures With Controlled Energy Absorption in the Hybrid Cellular Automaton Framework.* Journal of Mechanical Design, 2013. **135**(9): p. 091002-091002.
8. Shinde, S., et al., *Structural Optimization of Thin-Walled Tubular Structures for Progressive Buckling Using Compliant Mechanism Approach.* SAE International Journal of Passenger Cars - Mechanical Systems, 2013. **6**(1): p. 109-120.
9. Corporation, L.S.T., *LS-TaSC™ Topology and Shape Computations for LS-DYNA -- User's Manual*, ed. Lstc. 2011, Livermore, California.
10. Pedersen, C.B.W., *Topology optimization for crashworthiness of frame structures.* International Journal of Crashworthiness, 2003. **8**(1): p. 29-39.
11. Pedersen, C.B.W., *Crashworthiness design of transient frame structures using topology optimization.* Computer Methods in Applied Mechanics and Engineering, 2004. **193**(6-8): p. 653-678.
12. Kim, Y.-I. and G.-J. Park, *Nonlinear dynamic response structural optimization using equivalent static loads.* Computer Methods in Applied Mechanics and Engineering, 2010. **199**(9-12): p. 660-676.
13. Yi, S.I., J.Y. Lee, and G.J. Park, *Crashworthiness design optimization using equivalent static loads.* Proceedings of the Institution of Mechanical Engineers, Part D: Journal of Automobile Engineering, 2012. **226**(1): p. 23-38.
14. Jung, D.Y. and H.C. Gea, *Topology optimization of nonlinear structures.* Finite Elements in Analysis and Design, 2004. **40**(11): p. 1417-1427.
15. Mayer, R.R., N. Kikuchi, and R.A. Scott, *Application of topological optimization techniques to structural crashworthiness.* International Journal for Numerical Methods in Engineering, 1996. **39**(8): p. 1383-1403.
16. Soto, C.A., *Structural topology optimization for crashworthiness.* International Journal of Crashworthiness, 2004. **9**(3): p. 277-283.
17. Forsberg, J. and L. Nilsson, *Topology optimization in crashworthiness design.* Structural and Multidisciplinary Optimization, 2007. **33**(1): p. 1-12.
18. Penninger, C.L., et al., *Convergence analysis of hybrid cellular automata for topology optimization.* Structural and Multidisciplinary Optimization, 2010. **40**(1-6): p. 271-282.
19. Tovar, A. and K. Khandelwal, *Topology optimization for minimum compliance using a control strategy.* Engineering Structures, 2013. **48**: p. 674-682.
20. Patel, N.M., et al., *Comparative study of topology optimization techniques.* Aiaa Journal, 2008. **46**(8): p. 1963-1975.

21. Liu, K., et al., *Thin-walled compliant mechanism component design assisted by machine learning and multiple surrogates.* SAE International Journal of Passenger Cars – Mechanical Systems, 2015. **(in press)**.
22. Michell, A.G.M., *The Limits of Economy of Material in Frame-structures.* Philosophical Magazine S6, 1904. **8**(47): p. 589-597.